

1  
2  
3  
4  
5  
6  
7  
8  
9  
10  
11  
12  
13  
14  
15  
16  
17  
18  
19  
20  
21  
22  
23  
24  
25  
26  
27  
28  
29  
30  
31  
32  
33

**Porin-mediated small-molecule traffic across the outer membrane of Gram-negative bacteria**

Julia Vergalli<sup>1,#</sup>, Igor Bodrenko<sup>2,#</sup>, Muriel Masi<sup>1,#,§</sup>, Lucile Moynié<sup>3,4</sup>, Silvia Acosta-Gutiérrez<sup>2</sup>, James H. Naismith<sup>3,4</sup>, Anne Davin-Regli<sup>1</sup>, Matteo Ceccarelli<sup>2</sup>, Bert van den Berg<sup>5</sup>, Mathias Winterhalter<sup>6</sup>, Jean-Marie Pagès<sup>1,\*</sup>

<sup>1</sup> Aix Marseille Univ, INSERM, SSA, IRBA, MCT, Marseille 13005, France

<sup>2</sup> Department of Physics, University of Cagliari, and CNR/IOM, Cittadella Universitaria di Monserrato, 09042 Monserrato (CA).

<sup>3</sup> Division of Structural Biology, Nuffield Department of Medicine, 7 Roosevelt Drive, Oxford, OX3 7BN, United Kingdom.

<sup>4</sup> Rosalind Franklin Institute, Rutherford Laboratory, Didcot, OX11 0FA, United Kingdom

<sup>5</sup> Institute for Cell and Molecular Biosciences, The Medical School, Newcastle University, Newcastle upon Tyne NE2 4HH, United Kingdom.

<sup>6</sup> Department of Life Sciences and Chemistry, Jacobs University Bremen, 28719 Bremen, Germany.

# These authors contributed equally to this work

§ Present address: Institut de Biologie Intégrative de la Cellule (I2BC), Université Paris Sud, Orsay cedex, France.

\* Corresponding author

Jean-Marie Pagès,  
UMR\_MD1, INSERM-1261, Membranes et Cibles Thérapeutiques, Faculté de Pharmacie, 27 Bd Jean Moulin, 13385 Marseille cedex05, France.  
jean-marie.pages@univ-amu.fr

34 **Abstract**

35

36 Gram-negative bacteria and their complex cell envelope comprising an outer and  
37 inner membrane are an important and attractive system for studying the translocation  
38 of small molecules across biological membranes. In the outer membrane of  
39 *Enterobacteriaceae*, trimeric porins control the cellular penetration of small  
40 molecules, including nutrients and antibacterial agents. The synergistic action  
41 between relatively slow porin-mediated passive uptake across the outer membrane  
42 and active efflux transporters in the inner membrane creates a permeability barrier  
43 that re-inforces the enzymatic modification barrier, which efficiently reduces the  
44 intracellular concentrations of small molecules and contributes to the emergence of  
45 antibiotic resistance. In this review, we discuss recent advances in our understanding  
46 of the molecular and functional roles of classic porins in small molecule translocation  
47 in *Enterobacteriaceae* and consider the crucial role of porins in antibiotic resistance.

48

49

Commented [w1]: Is this specification necessary here?, in my opinion it deviates, better to put later...

Commented [JP2]: Editor request...

## 50 Introduction

51

52 Gram-negative bacteria have a complex cell envelope that comprises an outer  
53 membrane and an inner membrane, which together delineate the periplasmic space<sup>1-</sup>  
54 <sup>3</sup>. The inner or cytoplasmic membrane (IM) is a largely symmetrical phospholipid  
55 bilayer that is responsible for diverse physiological and metabolic functions. The  
56 outer membrane (OM) is the first line of defense, forming a physical/mechanical  
57 barrier that strongly protects the cell against external aggressive agents such as  
58 antibiotics, disinfectants, cationic peptides and bacteriocins<sup>2-4</sup>. The OM contains  
59 proteins that mediate the passive or active uptake of small molecules for growth and  
60 cell function<sup>4,5</sup>.

61 OM proteins form  $\beta$ -barrels composed of 8-22  $\beta$ -strands that have been  
62 characterized and classified according to their structure (monomeric or trimeric), their  
63 substrate specificity (e.g. specific diffusion channels for sugars like LamB) or mode of  
64 action, (e.g. active TonB-dependent transporters for metals and vitamins, like FhuA  
65 and BtuB, and general or classical porins for the non-specific diffusion of solutes with  
66 a molecular cutoff around 600 Da). Porins represent a substantial fraction of the total  
67 OM proteins in *Enterobacteriaceae* (> 10<sup>5</sup> copies/cell)<sup>4</sup>. *Escherichia coli* produces  
68 three major trimeric porins, namely OmpC and OmpF that exhibit selectivity for  
69 cationic molecules and PhoE with a preference to anionic molecules<sup>4,5</sup>.

70 OmpF and OmpC orthologs are present in closely related *Enterobacteriaceae*,  
71 including *Enterobacter aerogenes* now termed *Klebsiella aerogenes* (Omp35 and  
72 Omp36), *Enterobacter cloacae* (OmpEc35, OmpEc36) and *K. pneumoniae* (OmpK35  
73 and OmpK36)<sup>4,6</sup>. Besides their role as hydrophilic channels, porins contribute to  
74 membrane stability and participate in various physiological events of bacterial life.  
75 For example, they are major components of OM vesicles released by bacteria and  
76 can play a role during inflammation and response of the host immune system<sup>7-11</sup>.

77 They can also be involved in cell-cell contacts as reported for the *Providencia stuartii*  
78 OmpPst1<sup>12</sup>. In addition, OmpF is required during the entry of colicins and the cell-  
79 surface exposed loops of porins are involved in the colicin E3 translocation across  
80 the OM<sup>13</sup>.

81

82  $\beta$ -lactams and fluoroquinolones are the two prominent classes of antibiotics used in  
83 clinics for treating infections caused by Gram-negative pathogens<sup>2,3,6</sup>. Importantly,

84 porins represent the preferred route for the entry of  $\beta$ -lactams, including  
85 cephalosporins, penicillins and carbapenems<sup>14-16</sup>. The clinical relevance of  
86 membrane-associated mechanisms (MAMs) of resistance (*i.e.* porin defects and/or  
87 overexpression of multidrug efflux pumps<sup>5</sup>) has been well established for these  
88 antibiotics. The Influx and Efflux rates control the internal concentration of antibiotics  
89 and represent the first lane (mechanical barrier) protecting the bacterial cells against  
90 therapeutic treatment<sup>1-3,6</sup>. Consequently, studies on bacterial porins are receiving a  
91 renewed interest due to their key role in the bacterial susceptibility towards clinically  
92 used antibiotics. In combination with the expression of antibiotic-modifying enzymes  
93 expressed in the periplasm (e.g.  $\beta$ -lactamases), porins play a key role in  $\beta$ -lactam  
94 resistance<sup>4,17</sup>.

95  
96 In this review, we discuss recent advances in our understanding of the molecular and  
97 functional roles of classic porins in antibiotic translocation in *Enterobacteriaceae*. We  
98 explore structural aspects and the insights gained into permeation and the pore  
99 translocation process, the regulation of porin expression as well as the role of porins  
100 in the emergence of antibiotic susceptibility.

101

102

103

## 104 **Enterobacterial general porins**

### 105 ***Structural aspects***

106 The crystal structures of a general porin from *Rhodobacter capsulatus*<sup>18</sup>, the OmpF  
107 and PhoE porins from *E. coli*<sup>19</sup> and other *E. coli* OmpF structures including  
108 mutants<sup>20,21</sup> were the first to be solved. Only a limited number of other enterobacterial  
109 porin structures have been reported, *i.e.* *E. coli* OmpC, *K. pneumoniae* OmpK36 and  
110 *Salmonella typhi* OmpF<sup>22-24</sup>. The lack of data has hindered attempts to relate  
111 structure to function. Recently, the structures of two porins from *P. stuartii* as well as  
112 the structures of the OmpF and OmpC orthologs of *K. pneumoniae*, *E. aerogenes*  
113 and *E. cloacae* have been reported<sup>12,25,26</sup>. Another recent study reported that *E. coli*  
114 OmpF, OmpC and *K. pneumoniae* OmpK36 form complexes with MlaA, the  
115 phospholipid translocation channel component of the Mla system. The complex is  
116 critical to maintain the lipid asymmetry of the OM<sup>27</sup>. The X-ray crystal structures of *K.*

117 *pneumoniae* MlaA with OmpK36 and *E. coli* OmpF showed that MlaA is a pore-  
118 containing,  $\alpha$ -helical OM protein that selectively removes phospholipids from the  
119 outer OM leaflet<sup>28</sup>. As formation of a complex with MlaA does not seem to alter the  
120 structure of the porins, it seems likely that the porins function as scaffolds for MlaA  
121 and that their function is not affected by the bound lipoprotein. In this review we focus  
122 on porins as isolated molecules<sup>28</sup>.

123  
124 Porins are often organised as trimers, with inter-monomer contacts provided by the  
125 hydrophobic surfaces of the barrels and by extracellular loop L2, which latches into a  
126 groove of a neighbouring monomer and makes a number of polar interactions  
127 **(FIGURE 1)**. The trimer entity itself seems to have no clear function as no strong  
128 evidence has suggested that cooperativity exists within the trimer, *i.e.* the porin  
129 monomers likely function as independent subunits. The trimeric arrangement may  
130 simply confer additional stability. Viewed as a cross-section perpendicular to the  
131 membrane, the channels have an hourglass shape, with the narrowest part named  
132 "eyelet" or constriction region (CR, see FIGURE 1c, e). For *E. coli* OmpF and OmpC,  
133 the CR has a roughly circular shape with diameters of 6.5-7 Å and 5.5-6 Å  
134 respectively. The CR is the consequence of the presence of the ~35 residue-long  
135 extracellular loop L3, which folds inwards to generate a narrow pore (**FIGURE 1**);  
136 without it, the resulting huge pore of ~15 x 23 Å would severely compromise OM  
137 impermeability. Another, crucial consequence of the L3 loop is the generation of a  
138 strong (transverse) electric field across the CR, resulting from a row of positively  
139 charged residues on the barrel wall (K16, R37, R74 and R124 in *E. coli* OmpC) that  
140 lie opposite negatively charged residues (Asp105 and Glu109 in OmpC) and  
141 backbone carbonyl groups on L3 that point into the CR (**FIGURE 2**). This electric field  
142 has two important but distinct roles in controlling transport through the OM. First, it  
143 orients water molecules inside the pore, making it energetically unfavourable for  
144 hydrophobic small molecules to displace them and thus permeate through the CR.  
145 Second, the electric field has also direct consequences for the permeation of polar  
146 small molecules, as its shape and size have been shown to determine the efficiency  
147 with which molecules can pass the CR. The polarity in the CR also results in different  
148 permeation paths for simple anions relative to cations<sup>29</sup>. Although a large number of  
149 basic residues exposed into the eyelet region, both OmpF and OmpC with their  
150 orthologs are slightly cation selective, with a higher selectivity for OmpC-like porins

151 [\[REF Acosta ACS-ID 2018\]](#). In addition, the smaller size of OmpC-like porins  
152 determines a lower conductivity of ions with respect to OmpF-like porins. Early study  
153 showed that point mutations can alter in both direction permeability [\[REF Misra, R.,](#)  
154 [and Benson, S.A. \(1988\) Isolation and characterization of OmpC porin mutants with](#)  
155 [altered pore properties. J. Bacteriol. 170: 528-533\]](#). With the support of high  
156 resolution structures and modelling, the subtle perturbation of the electric field by  
157 mutation of residues was shown to be partly behind the development of clinical  
158 resistance<sup>30</sup>.

### 160 **Substrate specificity**

161 An important issue is the substrate specificity of general porins and the question  
162 whether these channels have *bona fide* binding sites for their substrates<sup>31</sup>. Early  
163 electrophysiological studies described transient current blockages of *E. coli* OmpF in  
164 the presence of various small molecules including antibiotics<sup>32</sup> suggesting weak  
165 binding sites in the vicinity of the CR. Obtaining structural confirmation for any  
166 potential binding sites has proven challenging, but the co-crystal structures for three  
167 antibiotics (ampicillin, carbenicillin and ertapenem) and *E. coli* OmpF were reported<sup>33</sup>.  
168 Importantly, the antibiotics occupy very different positions with ertapenem bound in  
169 the extracellular vestibule, ampicillin on the extracellular side of the CR and  
170 carbenicillin in the periplasmic vestibule. Notably, none of the compounds are bound  
171 in the CR, and only for ampicillin did the occupation of the observed binding site  
172 result in current blockages by computational electrophysiology<sup>33</sup>. Moreover, the  
173 structures were obtained with extremely high concentrations of antibiotics (1-2 M),  
174 *i.e.* at least four orders of magnitude higher than would likely be encountered *in vivo*.  
175 However, small decreases (up to 4-fold) in MIC values for *E. coli* were observed for  
176 selected single mutations of polar or charged residues in the ampicillin and  
177 carbenicillin binding sites. While these results suggest that disruption of a possible  
178 antibiotic binding site *increases* susceptibility, the very different locations of the sites  
179 raise some questions. An alternative and plausible explanation would be that the  
180 observed effects on antibiotic susceptibility are caused by local changes in the  
181 electrostatics of the channel, which would echo the observation that subtle changes  
182 in electrostatic properties can influence antibiotic permeation<sup>30</sup>. Thus, in terms of  
183 specificity, there is a clear difference between general porins and truly substrate-  
184 specific channels such as LamB and Tsx, where mM concentrations or lower are

Commented [MC3]: to reply to referee-1

185 sufficient to occupy substrate binding sites in crystal structures<sup>34,35</sup>. Nevertheless,  
186 mounting recent evidence clearly suggest that general porins are in part selective  
187 and allow passage of some compounds much more readily than others. Relating  
188 such preferential permeability to protein sequence would be powerful in designing  
189 antibiotics. A systematic study on the permeation of a series of antibiotics mediated  
190 by four OmpF/OmpC pairs (from *E. coli*, *K. pneumoniae*, *E. aerogenes* and *E.*  
191 *cloacae*) was reported recently<sup>25</sup>. This study showed that enterobacterial porin  
192 structures are topologically identical and even in detail very similar (**FIGURE 2**).  
193 However, analysis show that very subtle differences in structure lead to alteration of  
194 the electric field close to and within the constriction zone and are accompanied by  
195 differences in the permeation of antibiotics<sup>25</sup>. The new data allowed the development  
196 of a new quantitative scoring function for antibiotics permeation that is in broad  
197 agreement with *in vitro* permeation data. Thus, given a structure, it is now possible to  
198 predict what molecules are favored or disfavored in terms of permeation. Another  
199 recent study reported a set of more qualitative permeation rules, and used these to  
200 convert, via addition of an amine group, a narrow-spectrum compound (6-DNM) into  
201 a compound (6-DNM-NH<sub>3</sub>) that efficiently permeated *E. coli* as evidenced by 2 to 64-  
202 fold lower MIC values<sup>36</sup>. Interestingly, the data also showed lower MIC values for 6-  
203 DNM-NH<sub>3</sub> in *Pseudomonas aeruginosa* and *Acinetobacter baumannii*, despite the  
204 fact that these non-enteric pathogens lack general porins and instead possess  
205 substrate-specific channels. This in turn suggests that the structural properties that  
206 govern small-molecule permeation through *E. coli* porins may be, at least to some  
207 extent, broadly conserved in Gram-negative bacteria. While further work is certainly  
208 required, these studies provide clear hope for the design of more efficiently  
209 permeating antibiotics.

210

211

212

## 213 **Porin-mediated transport**

### 214 ***Experimental tools to characterize permeation across porins***

215 Early approaches to quantify small molecule uptake across Gram-negative cell  
216 envelopes revealed a correlation between the presence of porins and selective  
217 uptake across the outer cell wall. Isolation of porins and reconstitution into artificial

218 bilayers allowed conductance measurements to characterize single channels. In  
219 addition to ion selectivity, a statistical analysis of the conductance distribution  
220 suggested pore sizes of around one **nanometer**, close to that revealed by high  
221 resolution X-ray structures a few years later<sup>19</sup>.

222  
223 A complementary permeation technique was the so-called liposome swelling assay,  
224 whereby kinetic information on the uptake through the porins was obtained<sup>5</sup>. **Another**  
225 **method used to characterise indirectly the influx is to measure the endogenous**  
226 **periplasmic  $\beta$ -lactamase activity. Following the degradation product of antibiotics**  
227 **optically allowed to estimate their diffusion rate across OmpK35 and OmpK36 porin**  
228 **and showed a remarkably high permeability toward lipophilic (benzylpenicillin) and**  
229 **large (cefepime) compounds<sup>37</sup>. These results suggest a larger and more permeable**  
230 **channel for OmpK35 and OmpK36 than their *E. coli* homologs OmpF and OmpC**  
231 **explaining why drug resistance in *K. pneumoniae* caused by the loss of porins is**  
232 **often reported in clinical isolates<sup>37</sup>.**

233 **The recent technical breakthrough lead to ultrasensitive mass spectrometers allowing**  
234 **now whole cell accumulation assays. However, the sensitivity is not yet at single**  
235 **bacteria level and the crucial part in using the mass spectrometry method is to**  
236 **separate those molecules attached to the LPS outside of the cell from those that**  
237 **have truly penetrated<sup>36,38-44</sup>. For example, a study<sup>45</sup> revealed differences in**  
238 **ciprofloxacin accumulation between strains with efflux pumps compared to those with**  
239 **deactivated ones. Direct information on the accumulation of antibiotics in single**  
240 **bacterial cells<sup>45-47</sup> can be obtained using deep UV autofluorescence microscopy.**

241  
242 **A different method to characterize channel transport is to use the ion current as a**  
243 **probe for transport. Earlier work introduced the ion-current fluctuation to reveal on**  
244 **and off rates of sugar into the sugar-specific channel LamB<sup>48,49</sup>. This analysis requires**  
245 **a strong binding of the molecule inside the channel and once inside the binding site**  
246 **the molecule must sufficiently block the ion current<sup>50-54</sup>. Transferring this approach to**  
247 **other small molecules with low or no affinity to the channel is not straightforward.**  
248 **(see BOX 1 for more details).** A different approach involves the use of an unbalanced  
249 charge accumulation<sup>55,56</sup>. Creating a concentration gradient between both sides of  
250 the channel induces a concentration-driven flux (**BOX 2**). Unequal diffusion of the



251 charged compound versus the counterion created the so-called diffusion potential  
252 that can be easily recorded.

253

#### 254 ***The translocation process at atomic level***

255 Predicting the number of molecules per second that translocate through porins

256 (molecular flux) is a computationally and experimentally challenging task<sup>57</sup>. The

257 molecular flux is ultimately governed by the statistically averaged molecular  
258 interactions, or the free energy, of the molecule with the pore and the solvent water<sup>58</sup>.

259 The first MD simulation of OmpF in a fully solvated symmetric bilayer revealed the  
260 alignment of water molecules at the CR of the pore<sup>59</sup>, highlighting the already  
261 hypothesized existence of a strong electric field, transversal to the diffusion axis.

262 Later, MD and Brownian dynamics simulations have shown two distinct paths for  
263 diffusion of anions and cations<sup>60</sup>. OmpF selectivity was also studied by means of

264 macroscopic electrodiffusion models and the combination of molecular dynamics with  
265 electrophysiology experiments has started to elucidate the role of temperature and

266 pH in ion-selectivity for both OmpF and OmpC porins from *E. coli*<sup>61,62</sup>. This type of  
267 work emphasises the notion that the permeating ions interact with the wall of the  
268 channel and that ion movement does not follow simple diffusion. Further, for the

269 permeation of larger molecules such as antibiotics it is expected that the interaction  
270 with the surface of the channel is likely the rate-limiting factor. Cavity solvation  
271 energetics calculations in OmpC were used to infer compound permeability from its  
272 ability to replace favorable water molecules prior to ligand association<sup>63</sup>.

273 The first attempts to calculate the free energy interaction of the antibiotic with the  
274 pore surface applying advanced sampling techniques, such as metadynamics,  
275 allowed the identification of barriers and affinity sites close to the CR<sup>64</sup>. These studies

276 when combined with electrophysiology data suggested that favourable interactions in  
277 the CR correlate with enhanced diffusion through OmpF, introducing the binding site  
278 concept in the permeation problem<sup>64</sup>, supported by studies on site-directed  
279 mutagenesis of key residues in the CR affecting  $\beta$ -lactam influx and susceptibility<sup>5,65</sup>.

280 However, as pointed out, crystallographic studies showed that there is not a unique  
281 binding site inside OmpF<sup>33</sup>, and in the case of the zwitterionic ampicillin, its binding  
282 mode in the co-complex was not located in the CR but above it, in the so-called pre-  
283 orientation region<sup>66</sup>.

284

Commented [MC4]: Please cite again Ref Kullmann  
Biophys. J. 2002

285 The recent introduction of Graphic Processor Unit (GPU) for scientific computing  
 286 allowed extending the calculation of the antibiotic-pore interactions to the entire pore  
 287 length, opening the way to the introduction of the free energy landscape model to  
 288 rationalize the translocation process (see **BOX 2**). The simulations enabled  
 289 elucidation of the role of the main features of porin architecture on the diffusion of  
 290 dipolar molecules (**FIGURE 3**), showing how those molecules align their electric  
 291 dipole moment with the internal electrostatic field in the pore<sup>66,67</sup>, similar to water.  
 292 Moreover, the quantification of the electric field of porins, based on the analysis of  
 293 water polarization in all-atom simulations, confirmed that its largest component is  
 294 directed transversally to the axis of diffusion and is modulated by environmental  
 295 factors such as pH and salt concentrations<sup>68</sup>. The internal electric field of porins is  
 296 thus a key pore property that fine-tunes its selectivity filter and explains also why the  
 297 permeation rate of penicillins in OmpF decreases and becomes comparable to that in  
 298 OmpC at high salt concentrations, as observed experimentally<sup>69</sup>. ~~Subtle differences~~  
 299 ~~in electrostatics, due to mutations of charged OmpC residues in a series of clinical~~  
 300 ~~isolates, explain the different susceptibility of the mutated strains<sup>30</sup>.~~

301 The successful combination of electrophysiology, enhanced sampling techniques and  
 302 an improved excess noise statistical analysis made it possible to quantify the kinetic  
 303 parameters such as the residence time of molecules inside the pore<sup>70</sup> even well  
 304 below the resolution time of the apparatus<sup>71,72</sup>. Further, the permeation of norfloxacin  
 305 through OmpF demonstrated the existence of the transversal electric field and its  
 306 effect on the transport of dipolar molecules<sup>73</sup>. Finally, the permeation of three  $\beta$ -  
 307 lactamase inhibitors (avibactam, sulbactam and tazobactam) through OmpF and  
 308 OmpC orthologs from four enterobacterial species was recently characterised using  
 309 the charge unbalance method (**BOX 2**). **The experimental quantification of the**  
 310 **permeation rateflux** of molecules allowed to test and verify the free energy landscape  
 311 **model presented in Fig. 3**~~(described below ? or in Figure3?)~~: the main barrier in the  
 312 CR is caused by the pore's size reduction and for ions is low and broad whereas for  
 313 the  $\beta$ -lactam inhibitors is slightly higher but substantially narrower<sup>56</sup> because of  
 314 dipolar interactions with the electric field.

315

### 316 ***Molecular parameters controlling permeation***

317 Our knowledge about small molecule permeation in Gram-negative bacteria mostly  
 318 **came from the post-analyses of molecular properties of effective antibacterial**

Formatted: Strikethrough

**Commented [MC5]:** As suggested by Lucile, this is already stated in the first section, we can remove from here.

Formatted: Strikethrough

Formatted: Strikethrough

319 agents<sup>74-76</sup>, which have suggested polarity and molecular weight as key factors for  
320 determining permeation<sup>75</sup>. It is interesting to note how in the last two generations of  
321 cephalosporins all molecules are zwitterionic, with an additional positive group in the  
322 scaffold<sup>77</sup>. Only recent studies confirmed the importance of having a positive charge  
323 in the scaffold for a better penetration through cation-selective porins such as  
324 OmpF/OmpC<sup>73</sup>. In particular a systematic study on diverse molecular scaffolds (>150  
325 molecules), not necessarily with antimicrobial property, showed that the addition of an  
326 amine group can enhance accumulation in *E. coli*<sup>36</sup>. The new high-resolution X-ray  
327 structures of OmpF/OmpC orthologs from *Enterobacteriaceae*<sup>25</sup>, together with those  
328 obtained from *E. coli* clinical strains<sup>30</sup>, allowed a thorough computational  
329 investigation, which revealed the common filtering mechanism of general porins  
330 (FIGURE 3). From the systematic analysis of permeability data on nine clinically  
331 relevant antibiotics through the eight enterobacterial porins, it was shown that the  
332 main energetic barrier located in the CR along the diffusion axis ultimately regulates  
333 the molecular permeability. By incorporating this molecular mechanism in a scoring  
334 function (or a supervised machine learning algorithm), it was possible to predict  
335 molecular permeability through porins. The scoring function is based on two  
336 energetic terms,  $F_{steric} + F_{electrostatic}$ , which depend on the physico-chemical  
337 parameters of molecules, pores and solvents. It also suggests the following three  
338 useful conclusions about the molecular permeability through porins. First, the  
339 permeability is the ability to overcome a barrier, and hence, molecules need to be  
340 designed for their ability to pass the CR rather than to bind to the pore. Second, the  
341 parameters describing the molecules and the pores in the scoring function are  
342 obtained from statistical averages of physical observables along molecular dynamics  
343 simulations. Importantly, the steric term depends not only on the size of each  
344 molecule and on that of the pore but also on their fluctuations<sup>78</sup>. Thus, in many cases  
345 the permeation is only possible because the molecules and pores change their size  
346 due to spontaneous fluctuations induced by temperature. Third, although the size  
347 reduction of the pore in the CR accounts for the biggest part of the barrier ( $F_{steric}$ ), the  
348 electrostatic interaction ultimately shapes the barrier, either decreasing it or  
349 increasing it. Molecules with similar sizes can have very different permeabilities due  
350 to the electrostatic interactions with the pore. The reason is that the free energy  
351 barrier appears in the expression of permeability within an exponential function  
352 (Figure 3)<sup>58</sup>. Therefore, fine-tuning of charge distribution and thus the charge and

Commented [MC6]: Ok the ref 77 here

Commented [VJ7]: Ref 77 here, is it ok?

353 dipole moment of compounds should be considered when optimizing molecules for  
354 optimal permeability through porins<sup>66</sup>.

355

356

357

### 358 **Regulation of porin expression**

359 The regulation of classical porin expression in *Enterobacteriaceae* is complex  
360 (**SupplementaryInformation Figure**). Classical porin genes are transcribed as  
361 monocistronic mRNAs, which does not exclude co-regulation with other genes in  
362 their vicinity. Regulation of porin expression involves multiple genetic effectors and  
363 regulatory cascades<sup>79-85</sup>. These include transcriptional regulators of the XylS/AraC  
364 family, which are responsible for chemical stress responses; two-component systems  
365 (TCS), in which a sensor kinase in the IM detects a signal that is transmitted to a  
366 cytoplasmic regulator; and extracytoplasmic function (ECF) sigma factors, which can  
367 redirect some or all of the RNA polymerase to activate transcription. In particular,  
368 alternative sigma factor  $\sigma^E$  and TCS CpxAR contribute to the major envelope stress  
369 response (ESRs) pathways by detecting envelope alterations and modulating gene  
370 expression to limit the stress impact<sup>79,81,85</sup>. These ESRs have a common regulon and  
371 interconnections that can regulate similar gene expression in response to different  
372 stress. Importantly, both  $\sigma^E$  and Cpx regulate and are regulated by small regulatory  
373 RNAs (sRNAs) involved in the post-transcriptional response to envelope stress.

374

375 Due to their different channel properties and the role these play in OM permeability,  
376 the expression of OmpF and OmpC is tightly regulated by several factors (for recent  
377 reviews see<sup>6,16,65,81</sup>). Osmolarity is probably the best-understood environmental  
378 signal that modulates OmpF and OmpC expression via the EnvZ/OmpR TCS  
379 (**SupplementaryInformation Figure**)<sup>65</sup>. After activation by external signal, the  
380 phosphoryl group of autophosphorylated EnvZ is transferred to OmpR. Thus,  
381 phosphorylated OmpR (OmpR~P) acts as a transcription factor that differentially  
382 modulates the *ompF* and *ompC* expression. The *ompF* gene is transcribed at low  
383 osmolarity when the OmpR~P level is low and binds only the high-affinity binding  
384 sites present on *ompF*. Conversely, when the concentration of OmpR~P increases  
385 due to high osmolarity, OmpR~P occupies all binding sites available on *ompF* and

386 *ompC* and this sequential binding triggers the differential expression of the porin  
387 genes, e.g. increased transcription of *ompC* and repression of *ompF*.

388 Recent advances in RNA-based techniques<sup>86,87</sup> have increased our knowledge about  
389 the repertoire of bacterial sRNAs and their impact on OMP expression<sup>88-90</sup>.  
390 Importantly, sRNAs govern gene expression and allow a fast and efficient adjustment  
391 to different growth conditions. OmpF is post-transcriptionally repressed by the sRNA  
392 MicF. The control of the MicF sRNA expression depends on multiple signals and  
393 regulatory pathways<sup>91</sup>. This 93-nucleotide (nt) RNA is divergent to the *ompC* gene  
394 and acts by a direct base-pairing to a region that encompasses the ribosome binding  
395 site (RBS) and the start codon of the *ompF* mRNA, thus preventing the initiation of  
396 translation and favoring degradation<sup>92-94</sup>. Moreover, the positive regulation also  
397 includes EnvZ/OmpR in high osmolarity conditions, SoxS in response to oxidative  
398 stress and MarA in response to antibiotic stress<sup>95,96</sup>. More recently, a 109-nt MicC  
399 sRNA has been identified and is able to repress OmpC by a direct base-pairing to a  
400 5' untranslated region of the *ompC* mRNA<sup>97</sup>. Noteworthy, MicC is transcribed  
401 opposite to the *ompN* gene that encodes a quiescent porin and it has recently been  
402 reported that *ompN* and *micC* are submitted to complex regulation upon exposure to  
403  $\beta$ -lactam antibiotics<sup>98</sup>. This is consistent with *ompN-micC* and *ompC-micF* sharing a  
404 similar genetic organization and that *ompC* and *micF* are co-induced under specific  
405 conditions (i. e. high osmolarity via EnvZ/OmpR).

406  
407 The contribution of XylS/AraC transcriptional regulators in controlling envelope  
408 permeability has been known for some time. These include MarA that is the key  
409 transcriptional regulator encoded by the *marRAB* operon, RamA, SoxS and Rob,  
410 which synergistically contribute to decrease the antibiotic accumulation inside the  
411 bacterial cell via downregulation of porin genes and increase of antibiotic efflux via  
412 upregulation of multidrug efflux pumps such as AcrAB. MarRAB plays a central role  
413 in the enterobacterial response to external agents including antibiotics, detergents,  
414 disinfectants and preservatives<sup>6,99,100</sup>. In particular, MarA can inhibit porin expression  
415 - directly at the transcriptional level, through binding to a conserved Marbox in the  
416 promoter region of porin gene, and - indirectly at the post-transcriptional level by  
417 activating MicF (**SupplementaryInformation Figure**). Various point mutations  
418 and/or deletions in *marA* and *marR* have been reported in several clinical strains and  
419 contribute to the emergence of clinical MDR phenotypes<sup>65</sup>.

An additional regulator, RamA-RamR has been identified in *Enterobacter spp.*, *Klebsiella spp.*, *Salmonella spp.* but is absent in *Escherichia coli*<sup>6,16,99,100</sup>. RamA is able to directly enhance MarA transcription and a conserved marbox is detected in the two promoters of these genes. RamA is also able to control the expression of porins in *Enterobacter spp.* and *Klebsiella spp.*<sup>65,100,101</sup>.

## Porins and antibiotic susceptibility

### Porin expression (TABLE 1)

Several reports describe an alteration of porin expression (OmpF and OmpC) in *E. coli* clinical strains during antibiotherapy<sup>5</sup>. A recent study describes a point mutation in the OmpR regulator that induces a conformational change involved in the repression of porin gene expression and thus in carbapenem resistance<sup>102</sup>. Moreover, in various collections of carbapenem non-susceptible *Enterobacteriaceae*, porin expression correlates with the level of carbapenem resistance<sup>103</sup>. This porin-susceptibility relationship seems to be associated with the characteristics of the porin channel, (OmpC type versus OmpF type), as recently discussed for  $\beta$ -lactam class compounds<sup>6,25,67</sup>. In *P. stuartii*, a defect of OmpPst1 expression or the presence of mutations in the corresponding gene have been described in resistant clinical strains<sup>104,105</sup>. These mutations are located in extracellular loops, which might be involved in trimer flexibility and may contribute to the active conformation of the porin<sup>12,105</sup>. Regarding *K. pneumoniae*, *E. cloacae* and *E. aerogenes*, the development of drug resistance is often found associated with a reduced level of porin expression or the mutational loss of its major porins<sup>103,106-109</sup>. Similarly, *Salmonella enterica* serovar Typhimurium developed carbapenem resistance during ertapenem treatment due to an OmpC deficiency<sup>110</sup>. Drug resistance in *Enterobacteriaceae* is mostly caused by lack of or reduced expression of the major porins combined with various  $\beta$ -lactamases and efflux pumps expressions: these mechanisms cooperate to strongly decrease the level of active antibiotic in the periplasm<sup>103,111-115</sup>. The efficiency of efflux pumps and  $\beta$ -lactamases is strongly increased because in porin-deficient cells the concentrations of antibiotics in periplasm are below the saturation levels of enzymes and transporters (BOX 3). Consequently, porin deficiency has been reported in clinical isolates of extended-

454 spectrum  $\beta$ -lactamases (ESBL)-producing *Enterobacteriaceae* resistant to other  
 455 compounds, such as quinolones<sup>116</sup>.

456 Importantly, a whole genome sequencing study combined with phenotypic and  
 457 biochemical characterizations has demonstrated the sequential emergence of target  
 458 mutations associated with alteration of porin expression in *E. aerogenes* isolates  
 459 collected during antibiotic treatments of two patients<sup>107</sup>.

460 The sequential replacement of expressed porin (OmpF substituted by OmpC family  
 461 expression) results in reduced influx and correlates with the resistance phenotype  
 462 observed in *Enterobacteriaceae* isolates: susceptible isolates express both major  
 463 porins, low level / intermediate resistant isolates exhibit one truncated porin, and the  
 464 loss of both major porins leads to the highest level of resistance with a complete  
 465 impermeability to  $\beta$ -lactams<sup>6,65,107,111,117-120</sup>. It was also reported that the expression  
 466 of a truncated OmpK36 during carbapenem treatment provided a wider spectrum of  
 467 resistance<sup>121,122</sup>. Other mutations in *ompK35* and *ompK36* have been reported as the  
 468 most likely contributor to ceftazidime-avibactam resistance in several *K. pneumoniae*  
 469 strains<sup>123-126</sup>. The reported mutations directly affect the porin expression or, due to  
 470 their location in the OmpK36 internal loop, affect the activity of imipenem-relebactam  
 471 or meropenem-varbobactam combinations<sup>127,128</sup>.

472

#### 473 **Mutation in the porin CR (TABLE 1)**

474 *Enterobacteriaceae* isolates express variants of OmpC orthologs resulting from the  
 475 substitution or insertion of one or two amino acids in loop L3 at or near the CR of the  
 476 porin channel (FIGURE 1). Gly->Asp substitution located in the PEFXGD motif of the  
 477 L3 loop<sup>5</sup> was detected in  $\beta$ -lactam resistant isolates of *E. aerogenes* and *K.*  
 478 *pneumoniae*<sup>129-131</sup>. An OmpK36 variant, exhibiting two additional amino acids  
 479 (Asp137 and Thr138) in the loop, shows both ertapenem resistance and a reduced  
 480 meropenem susceptibility<sup>132</sup>. The conserved PEFXGD motif forms a turn in the L3  
 481 loop and so contribute to the formation of the CR. Interestingly, the mutation Gly-  
 482 >Asp in this domain is also involved in ceftazidime-varbobactam resistance<sup>128</sup>.

483 Several other studies have reported a similar variant of OmpK36 with insertion of  
 484 either Asp-Gly or Gly-Asp in L3, conferring a resistance to carbapenem<sup>114,133-136</sup>.  
 485 OmpC mutants in *E. coli* clinical strains present diverse mutations in the channel  
 486 constriction that perturb the transverse electric field in CR without reducing its size,  
 487 thus trapping the drug in an orientation unfavorable for permeation<sup>30,67</sup>.

Commented [JP8]: this is clinical observation

488 Consequently, the translocation efficacy of antibiotic across the channel is  
489 decreased, providing reduced periplasmic accumulation and a decrease in  $\beta$ -lactam  
490 susceptibilities, independent of porin expression levels<sup>5</sup>. **Importantly, this reduced**  
491 **internal amount is associated with an induction of  $\beta$ -lactamase expression<sup>128</sup>.**  
492

### 493 **Alternative porins**

494 *Enterobacteriaceae* are able to express alternative porins to balance the loss of  
495 classical porins<sup>5,123</sup>. Overexpression of LamB has been reported in resistant isolates  
496 of *E. aerogenes* and *K. pneumoniae* yielding to a reduced antibiotic susceptibility  
497 while preserving bacterial fitness<sup>5,65,137</sup>. A correlation between phosphoporin PhoE  
498 expression and carbapenem susceptibility has been reported in clinical isolates of *K.*  
499 *pneumoniae* devoid of OmpK35 and OmpK36. The first isolate displayed  
500 carbapenem resistance, the second was susceptible to all carbapenems due to its  
501 constitutive expression of PhoE, and the third isolate was resistant to ertapenem and  
502 cefoxitin but susceptible to imipenem since it expressed PhoE at a low level<sup>138</sup>. No  
503 fitness alteration for the two PhoE expressing isolates was observed. Downregulation  
504 of PhoE has also been previously observed in carbapenem resistant *K. pneumoniae*  
505 isolates<sup>139</sup>. Interestingly **the expression of** OmpK26 porin, which usually transports  
506 acidic oligosaccharides, confers carbapenem low susceptibility in the absence of  
507 OmpK36 in a *K. pneumoniae* isolate<sup>137</sup>. However, this OmpK26 expression does not  
508 restore the fitness due to OmpK36 loss<sup>137</sup>. *K. pneumoniae* can also induce the  
509 expression of the quiescent porin OmpK37 (the ortholog of *E. coli* OmpN) to maintain  
510 its fitness<sup>140</sup> but this porin seems to play only a minor role in  $\beta$ -lactam  
511 resistance<sup>111,139-141</sup>.

512

513

514

### 515 **Concluding remarks**

516 The regulation of porin expression involves several modes of regulation. In addition,  
517 the final assembly as functional trimers into the OM is tightly controlled by the BAM  
518 machinery but also requires LPS binding<sup>26,142-144</sup>. These complex and partly  
519 redundant systems efficiently control the production of porins, which represent a  
520 prominent part of the OM protein landscape and are directly involved in OM  
521 permeability. The regulation systems are also responsible for a rapid adaptation



522 following external stresses such as antibiotics, chemicals, and colicins<sup>1,6</sup>. It should be  
523 stressed that only few studies have studied a possible role of MicF and MicC in the  
524 alteration of OM permeability in resistant strains<sup>145-147</sup>. To define the contribution of  
525 sRNA post-transcriptional silencing of porin genes in the regulation of porins, it  
526 seems important to investigate this aspect in addition to other regulators (MarA,  
527 RamA, etc) in clinical isolates during antibiotic treatment. It is also important to  
528 consider all flux across bacterial membranes (Influx and Efflux) as a continuum that  
529 controls the internal concentration of drugs via a coordinated regulation of  
530 transporter/porin expression.

531  
532 The internal conserved architecture of the channel inside the CR with its distribution  
533 of negative and positive charges and resulting electrostatic field is the strategic check  
534 point controlling the entrance of small polar compounds. In this key region, several  
535 specific mutations can alter the channel properties and increase or decrease the  
536 influx rate of molecules across the OM (for recent reviews see <sup>6,65</sup>).

537 Since porin channels represent an Achilles heel in the membrane barrier that  
538 protects the bacterial cell against toxic external compounds, it is not surprising that  
539 the loss of porin has often been reported in resistant clinical isolates. While allowing  
540 the bacteria to grow during antibiotherapy, the deficiency of major porins has a  
541 significant effect on the fitness and virulence of these resistant isolates.  
542 Consequently, clinical isolates encoding altered but still functional porins or alternate  
543 porins might have an advantage over isolates with non-functional porins. This  
544 strategy generates a minimal fitness cost for the bacterial cell while at the same time  
545 decreasing antibiotic susceptibility, which would contribute to the selection and the  
546 successful spread of resistant phenotype isolates.

547  
548 Recent technical advances allow measuring the rate of compound accumulation  
549 inside individual bacterial cells and the translocation through reconstituted porin  
550 channels *in vitro*, the simulation of the journey of small molecules inside the pore,  
551 and the pharmacomodulation of new pore-permeating compounds. These advances  
552 will undoubtedly help us to understand the translocation of drugs across bacterial  
553 membranes and will enable the design-improved molecules with better penetration  
554 and accumulation within Gram-negative bacteria.

555

556

557

558

**559 Acknowledgments**

560 We gratefully acknowledge R. A. Stavenger for the stimulating and helpful  
561 discussions during this work. The research leading to these results was conducted as  
562 part of the TRANSLOCATION consortium, and it has received support from the  
563 Innovative Medicines Initiatives Joint Undertaking under Grant Agreement n°115525  
564 (TRANSLOCATION) resources which are composed of financial contribution from the  
565 European Union's seventh framework program (FP7/2007-2013) and EFPIA  
566 companies in kind contribution. JM. Pagès was also partially supported by Aix-  
567 Marseille Univ. and Service de Santé des Armées, INSERM. M. Ceccarelli was  
568 partially supported by the Italian MIUR, PRIN Project 2015795S5W\_005. [L. Moynie](#)  
569 [was also supported ND4BB ENABLE Consortium and it has received support from](#)  
570 [the Innovative Medicines Initiatives Joint Undertaking under Grant Agreement](#)  
571 [n°115583.](#) We apologize to those whose papers and studies are not cited owing to  
572 space limitation.

573

574

575

576 **REFERENCES**

577

- 578 1. Nikaido, H. Outer membrane barrier as a mechanism of antimicrobial resistance.  
579 *Antimicrob Agents Chemother* **33**, 1831–1836 (1989).
- 580 2. Zgurskaya, H. I., López, C. A. & Gnanakaran, S. Permeability barrier of Gram-  
581 negative cell envelopes and approaches to bypass it. *ACS Infect Dis* **1**, 512–522  
582 (2015).
- 583 3. Hancock, R. E. W. The bacterial outer membrane as a drug barrier. *Trends in*  
584 *Microbiology* **5**, 37–42 (1997).
- 585 4. Nikaido, H. Molecular basis of bacterial outer membrane permeability revisited.  
586 *Microbiol Mol Biol Rev* **67**, 593–656 (2003).
- 587 5. Pagès, J.-M., James, C. E. & Winterhalter, M. The porin and the permeating  
588 antibiotic: a selective diffusion barrier in Gram-negative bacteria. *Nat Rev Micro*  
589 **6**, 893–903 (2008).
- 590 6. Masi, M., Réfrégiers, M., Pos, K. M. & Pagès, J.-M. Mechanisms of envelope  
591 permeability and antibiotic influx and efflux in Gram-negative bacteria. *Nature*  
592 *Microbiology* **2**, 17001 (2017).
- 593 7. Yan, J. J., Wang, M. C., Zheng, P. X., Tsai, L. H. & Wu, J. J. Associations of the  
594 major international high-risk resistant clones and virulent clones with specific  
595 *ompK36* allele groups in *Klebsiella pneumoniae* in Taiwan. *New Microbes New*  
596 *Infect* **5**, 1–4 (2015).
- 597 8. Galdiero, S. *et al.* Microbe-host interactions: Structure and role of Gram-negative  
598 bacterial porins. *Curr Protein Pept Sci* **13**, 843–854 (2012).
- 599 9. Liu, Y.-F. *et al.* Loss of outer membrane protein C in *Escherichia coli* contributes  
600 to both antibiotic resistance and escaping antibody-dependent bactericidal  
601 activity. *Infect Immun* **80**, 1815–1822 (2012).
- 602 10. Salerno-Gonçalves, R. *et al.* Use of a novel antigen expressing system to study  
603 the *Salmonella enterica* serovar Typhi protein recognition by T cells. *PLoS Negl*  
604 *Trop Dis* **11**, (2017).
- 605 11. Pérez-Toledo, M. *et al.* *Salmonella* Typhi porins OmpC and OmpF are potent  
606 adjuvants for T-dependent and T-independent antigens. *Front Immunol* **8**, (2017).

- 607 12. El-Khatib, M. *et al.* Porin self-association enables cell-to-cell contact in  
608 *Providencia stuartii* floating communities. *Proc Natl Acad Sci U S A* **115**, E2220–  
609 E2228 (2018).
- 610 13. Cramer, W. A., Sharma, O. & Zakharov, S. D. On mechanisms of colicin import:  
611 the outer membrane quandary. *Biochemical Journal* **475**, 3903–3915 (2018).
- 612 14. Walsh, C. *Antibiotics: actions, origins, resistance*. (American Society of  
613 Microbiology, 2003). doi:10.1128/9781555817886
- 614 15. Bryskier. *Antimicrobial Agents: Antibacterials and Antifungals*. (American Society  
615 of Microbiology, 2005). doi:10.1128/9781555815929
- 616 16. Dam, S., Pagès, J.-M. & Masi, M. Stress responses, outer membrane  
617 permeability control and antimicrobial resistance in *Enterobacteriaceae*.  
618 *Microbiology* **164**, 260–267 (2018).
- 619 17. Bush, K. Past and present perspectives on  $\beta$ -lactamases. *Antimicrobial Agents*  
620 *and Chemotherapy* **62**, e01076-18 (2018).
- 621 18. Weiss, M. S. & Schulz, G. E. Structure of porin refined at 1.8 Å resolution. *Journal*  
622 *of Molecular Biology* **227**, 493–509 (1992).
- 623 19. Cowan, S. W. *et al.* Crystal structures explain functional properties of two *E. coli*  
624 porins. *Nature* **358**, 727 (1992).
- 625 20. Lou, K.-L. *et al.* Structural and functional characterization of OmpF porin mutants  
626 selected for larger pore size. I. CRYSTALLOGRAPHIC ANALYSIS. *J. Biol.*  
627 *Chem.* **271**, 20669–20675 (1996).
- 628 21. Phale, P. S. *et al.* Role of charged residues at the OmpF porin channel  
629 constriction probed by mutagenesis and simulation. *Biochemistry* **40**, 6319–6325  
630 (2001).
- 631 22. Baslé, A., Rummel, G., Storici, P., Rosenbusch, J. P. & Schirmer, T. Crystal  
632 structure of osmoporin OmpC from *E. coli* at 2.0 Å. *Journal of Molecular Biology*  
633 **362**, 933–942 (2006).
- 634 23. Dutzler, R. *et al.* Crystal structure and functional characterization of OmpK36, the  
635 osmoporin of *Klebsiella pneumoniae*. *Structure* **7**, 425–434 (1999).
- 636 24. Balasubramaniam, D., Arockiasamy, A., Kumar, P. D., Sharma, A. &  
637 Krishnaswamy, S. Asymmetric pore occupancy in crystal structure of OmpF porin  
638 from *Salmonella typhi*. *Journal of Structural Biology* **178**, 233–244 (2012).

- 639 25. Acosta-Gutiérrez, S. *et al.* Getting drugs into Gram-negative bacteria: Rational  
640 rules for permeation through general porins. *ACS Infect Dis* **4**, 1487–1498 (2018).
- 641 26. Arunmanee, W. *et al.* Gram-negative trimeric porins have specific LPS binding  
642 sites that are essential for porin biogenesis. *PNAS* **113**, E5034–E5043 (2016).
- 643 27. Malinverni, J. C. & Silhavy, T. J. An ABC transport system that maintains lipid  
644 asymmetry in the gram-negative outer membrane. *Proc. Natl. Acad. Sci. U.S.A.*  
645 **106**, 8009–8014 (2009).
- 646 28. Abellón-Ruiz, J. *et al.* Structural basis for maintenance of bacterial outer  
647 membrane lipid asymmetry. *Nature Microbiology* **2**, 1616 (2017).
- 648 29. Dhakshnamoorthy, B., Ziervogel, B. K., Blachowicz, L. & Roux, B. A structural  
649 study of ion permeation in OmpF porin from anomalous X-ray diffraction and  
650 molecular dynamics simulations. *J. Am. Chem. Soc.* **135**, 16561–16568 (2013).
- 651 30. Lou, H. *et al.* Altered antibiotic transport in OmpC mutants isolated from a series  
652 of clinical strains of multi-drug resistant *E. coli*. *PLoS One* **6**, (2011).
- 653 31. Kojima, S. & Nikaido, H. Permeation rates of penicillins indicate that *Escherichia*  
654 *coli* porins function principally as nonspecific channels. *PNAS* **110**, E2629–E2634  
655 (2013).
- 656 32. Nestorovich, E. M., Danelon, C., Winterhalter, M. & Bezrukov, S. M. Designed to  
657 penetrate: Time-resolved interaction of single antibiotic molecules with bacterial  
658 pores. *PNAS* **99**, 9789–9794 (2002).
- 659 33. Ziervogel, B. K. & Roux, B. The binding of antibiotics in OmpF porin. *Structure* **21**,  
660 76–87 (2013).
- 661 34. Dutzler, R., Wang, Y.-F., Rizkallah, P. J., Rosenbusch, J. P. & Schirmer, T.  
662 Crystal structures of various maltooligosaccharides bound to maltoporin reveal a  
663 specific sugar translocation pathway. *Structure* **4**, 127–134 (1996).
- 664 35. Ye, J. & van den Berg, B. Crystal structure of the bacterial nucleoside transporter  
665 Tsx. *EMBO J* **23**, 3187–3195 (2004).
- 666 36. Richter, M. F. *et al.* Predictive compound accumulation rules yield a broad-  
667 spectrum antibiotic. *Nature* **545**, 299–304 (2017).
- 668 37. Sugawara, E., Kojima, S. & Nikaido, H. *Klebsiella pneumoniae* major porins  
669 OmpK35 and OmpK36 allow more efficient diffusion of  $\beta$ -lactams than their  
670 *Escherichia coli* homologs OmpF and OmpC. *J Bacteriol* **198**, 3200–3208 (2016).

- 671 38. Cai, H., Rose, K., Liang, L.-H., Dunham, S. & Stover, C. Development of a liquid  
672 chromatography/mass spectrometry-based drug accumulation assay in  
673 *Pseudomonas aeruginosa*. *Analytical Biochemistry* **385**, 321–325 (2009).
- 674 39. Schumacher, A. *et al.* Intracellular accumulation of linezolid in *Escherichia coli*,  
675 *Citrobacter freundii* and *Enterobacter aerogenes*: role of enhanced efflux pump  
676 activity and inactivation. *J Antimicrob Chemother* **59**, 1261–1264 (2007).
- 677 40. Davis, T. D., Gerry, Christopher J. & Tan, D. S. General platform for systematic  
678 quantitative evaluation of small-molecule permeability in bacteria. *ACS Chem Biol*  
679 **9**, 2535–2544 (2014).
- 680 41. Zhou, Y. *et al.* Thinking outside the “Bug”: A unique assay to measure  
681 intracellular drug penetration in Gram-negative bacteria. *Anal. Chem.* **87**, 3579–  
682 3584 (2015).
- 683 42. Iyer, R. *et al.* Evaluating LC-MS/MS to measure accumulation of compounds  
684 within bacteria. *ACS Infect Dis* **4**, 1336–1345 (2018).
- 685 43. Six, D. A., Krucker, T. & Leeds, J. A. Advances and challenges in bacterial  
686 compound accumulation assays for drug discovery. *Current Opinion in Chemical*  
687 *Biology* **44**, 9–15 (2018).
- 688 44. Prochnow, H. *et al.* Subcellular quantification of uptake in Gram-negative  
689 bacteria. *Anal. Chem.* **91**, 1863–1872 (2019).
- 690 45. Vergalli, J. *et al.* Fluoroquinolone structure and translocation flux across bacterial  
691 membrane. *Scientific Reports* **7**, 9821 (2017).
- 692 46. Vergalli, J. *et al.* Spectrofluorimetric quantification of antibiotic drug concentration  
693 in bacterial cells for the characterization of translocation across bacterial  
694 membranes. *Nature Protocols* **13**, 1348–1361 (2018).
- 695 47. Allam, A. *et al.* Microspectrofluorimetry to dissect the permeation of ceftazidime in  
696 Gram-negative bacteria. *Sci Rep* **7**, (2017).
- 697 48. Andersen, C., Jordy, M. & Benz, R. Evaluation of the rate constants of sugar  
698 transport through maltoporin (LamB) of *Escherichia coli* from the sugar-induced  
699 current noise. *J Gen Physiol* **105**, 385–401 (1995).
- 700 49. Kullman, L., Winterhalter, M. & Bezrukov, S. M. Transport of maltodextrins  
701 through maltoporin: a single-channel study. *Biophys J* **82**, 803–812 (2002).
- 702 50. Gutschmann, T., Heimburg, T., Keyser, U., Mahendran, K. R. & Winterhalter, M.  
703 Protein reconstitution into freestanding planar lipid membranes for  
704 electrophysiological characterization. *Nature Protocols* **10**, 188–198 (2015).

- 705 51. Mahendran, K. R., Kreir, M., Weingart, H., Fertig, N. & Winterhalter, M.  
706 Permeation of antibiotics through *Escherichia coli* OmpF and OmpC porins:  
707 Screening for influx on a single-molecule level. *J Biomol Screen* **15**, 302–307  
708 (2010).
- 709 52. Mahendran, K. R. *et al.* Molecular basis of enrofloxacin translocation through  
710 OmpF, an outer membrane channel of *Escherichia coli* - When binding does not  
711 imply translocation. *J. Phys. Chem. B* **114**, 5170–5179 (2010).
- 712 53. Singh, P. R., Ceccarelli, M., Lovelle, M., Winterhalter, M. & Mahendran, K. R.  
713 Antibiotic permeation across the OmpF channel: Modulation of the affinity site in  
714 the presence of magnesium. *Journal of Physical Chemistry B* **116**, 4433–4438  
715 (2012).
- 716 54. Wang, J., Bafna, J. A., Bhamidimarri, S. P. & Winterhalter, M. Small-molecule  
717 permeation across membrane channels: Chemical modification to quantify  
718 transport across OmpF. *Angewandte Chemie International Edition* **58**, 4737–4741  
719 (2019).
- 720 55. Ghai, I. *et al.* Ampicillin permeation across OmpF, the major outer-membrane  
721 channel in *Escherichia coli*. *J. Biol. Chem.* **293**, 7030–7037 (2018).
- 722 56. Ghai, I. *et al.* General method to determine the flux of charged molecules through  
723 nanopores applied to  $\beta$ -lactamase inhibitors and OmpF. *J. Phys. Chem. Lett.* **8**,  
724 1295–1301 (2017).
- 725 57. Winterhalter, M. & Ceccarelli, M. Physical methods to quantify small antibiotic  
726 molecules uptake into Gram-negative bacteria. *European Journal of*  
727 *Pharmaceutics and Biopharmaceutics* **95**, 63–67 (2015).
- 728 58. Scorciapino, M. A. *et al.* Rationalizing the permeation of polar antibiotics into  
729 Gram-negative bacteria. *J. Phys.: Condens. Matter* **29**, 113001 (2017).
- 730 59. Tieleman, D. P. & Berendsen, H. J. A molecular dynamics study of the pores  
731 formed by *Escherichia coli* OmpF porin in a fully hydrated  
732 palmitoylcholine bilayer. *Biophys J* **74**, 2786–2801 (1998).
- 733 60. Im, W. & Roux, B. Ion permeation and selectivity of OmpF porin: A theoretical  
734 study based on molecular dynamics, brownian dynamics, and continuum  
735 electrodiffusion theory. *Journal of Molecular Biology* **322**, 851–869 (2002).

- 736 61. Aguilera-Arzo, M., García-Celma, J. J., Cervera, J., Alcaraz, A. & Aguilera, V. M.  
737 Electrostatic properties and macroscopic electrodiffusion in OmpF porin and  
738 mutants. *Bioelectrochemistry* **70**, 320–327 (2007).
- 739 62. Biró, I., Pezeshki, S., Weingart, H., Winterhalter, M. & Kleinekathöfer, U.  
740 Comparing the temperature-dependent conductance of the two structurally similar  
741 *E. coli* porins OmpC and OmpF. *Biophysical Journal* **98**, 1830–1839 (2010).
- 742 63. Tran, Q.-T., Williams, S., Farid, R., Erdemli, G. & Pearlstein, R. The translocation  
743 kinetics of antibiotics through porin OmpC: Insights from structure-based  
744 solvation mapping using WaterMap. *Proteins: Structure, Function, and*  
745 *Bioinformatics* **81**, 291–299 (2013).
- 746 64. Ceccarelli, M., Danelon, C., Laio, A. & Parrinello, M. Microscopic mechanism of  
747 antibiotics translocation through a porin. *Biophysical Journal* **87**, 58–64 (2004).
- 748 65. Masi, M., Pagès, J.-M. & Winterhalter, M. Outer membrane porins. in *Bacterial*  
749 *Cell Walls and Membranes* 1–54 (A. Kuhn, 2019).
- 750 66. Acosta-Gutierrez, S., Scorciapino, M. A., Bodrenko, I. & Ceccarelli, M. Filtering  
751 with electric field: The case of *E. coli* porins. *J. Phys. Chem. Lett.* **6**, 1807–1812  
752 (2015).
- 753 67. Bajaj, H. *et al.* Molecular basis of filtering carbapenems by porins from  $\beta$ -lactam-  
754 resistant clinical strains of *Escherichia coli*. *J. Biol. Chem.* **291**, 2837–2847  
755 (2016).
- 756 68. Acosta-Gutierrez, S., Bodrenko, I., Scorciapino, M. A. & Ceccarelli, M.  
757 Macroscopic electric field inside water-filled biological nanopores. *Phys. Chem.*  
758 *Chem. Phys.* **18**, 8855–8864 (2016).
- 759 69. Kojima, S. & Nikaido, H. High salt concentrations increase permeability through  
760 OmpC channels of *Escherichia coli*. *J. Biol. Chem.* **289**, 26464–26473 (2014).
- 761 70. D'Agostino, T., Salis, S. & Ceccarelli, M. A kinetic model for molecular diffusion  
762 through pores. *Biochimica et Biophysica Acta (BBA) - Biomembranes* **1858**,  
763 1772–1777 (2016).
- 764 71. Bodrenko, I., Bajaj, H., Ruggerone, P., Winterhalter, M. & Ceccarelli, M. Analysis  
765 of fast channel blockage: revealing substrate binding in the microsecond range.  
766 *Analyst* **140**, 4820–4827 (2015).



- 767 72. Bodrenko, I. V., Wang, J., Salis, S., Winterhalter, M. & Ceccarelli, M. Sensing  
768 single molecule penetration into nanopores: Pushing the time resolution to the  
769 diffusion limit. *ACS Sens* **2**, 1184–1190 (2017).
- 770 73. Bajaj, H. *et al.* Bacterial outer membrane porins as electrostatic nanosieves:  
771 Exploring transport rules of small polar molecules. *ACS Nano* **11**, 5465–5473  
772 (2017).
- 773 74. Payne, D. J., Gwynn, M. N., Holmes, D. J. & Pompliano, D. L. Drugs for bad  
774 bugs: confronting the challenges of antibacterial discovery. *Nature Reviews Drug*  
775 *Discovery* **6**, 29–40 (2007).
- 776 75. O'Shea, R. & Moser, H. E. Physicochemical properties of antibacterial  
777 compounds: Implications for drug discovery. *J. Med. Chem.* **51**, 2871–2878  
778 (2008).
- 779 76. Brown, D. G., May-Dracka, T. L., Gagnon, M. M. & Tommasi, R. Trends and  
780 exceptions of physical properties on antibacterial activity for Gram-positive and  
781 Gram-negative pathogens. *J. Med. Chem.* **57**, 10144–10161 (2014).
- 782 77. Page, M. G. P. Beta-lactam antibiotics. in *Antibiotic Discovery and Development*  
783 79–117 (Dougherty, T. J., and Pucci, M., Eds., 2011).
- 784 78. Bodrenko, I. V., Salis, S., Acosta-Gutierrez, S. & Ceccarelli, M. Diffusion of large  
785 particles through small pores: from entropic to enthalpic transport. *J. Chem. Phys.*  
786 **150**, 211102–211106 (2019).
- 787 79. Grabowicz, M. & Silhavy, T. J. Envelope stress responses: An interconnected  
788 safety net. *Trends Biochem Sci* **42**, 232–242 (2017).
- 789 80. Chen, H. D. & Groisman, E. A. The biology of the PmrA/PmrB two-component  
790 system: The major regulator of lipopolysaccharide modifications. *Annual Review*  
791 *of Microbiology* **67**, 83–112 (2013).
- 792 81. Guest, R. L. & Raivio, T. L. Role of the Gram-negative envelope stress response  
793 in the presence of antimicrobial agents. *Trends in Microbiology* **24**, 377–390  
794 (2016).
- 795 82. Zschiedrich, C. P., Keidel, V. & Szurmant, H. Molecular mechanisms of two-  
796 component signal transduction. *J Mol Biol* **428**, 3752–3775 (2016).
- 797 83. Laloux, G. & Collet, J.-F. Major Tom to ground control: How lipoproteins  
798 communicate extracytoplasmic stress to the decision center of the cell. *J*  
799 *Bacteriol* **199**, (2017).

- 800 84. Tiwari, S. *et al.* Two-component signal transduction systems of pathogenic  
801 bacteria as targets for antimicrobial therapy: An overview. *Front Microbiol* **8**,  
802 (2017).
- 803 85. Fröhlich, K. S. & Gottesman, S. Small regulatory RNAs in the enterobacterial  
804 response to envelope damage and oxidative stress. *Microbiology Spectrum* **6**,  
805 (2018).
- 806 86. Barquist, L. & Vogel, J. Accelerating discovery and functional analysis of small  
807 RNAs with new technologies. *Annual Review of Genetics* **49**, 367–394 (2015).
- 808 87. Vogel, J. & Wagner, E. G. H. Target identification of small noncoding RNAs in  
809 bacteria. *Current Opinion in Microbiology* **10**, 262–270 (2007).
- 810 88. Guillier, M., Gottesman, S. & Storz, G. Modulating the outer membrane with small  
811 RNAs. *Genes Dev.* **20**, 2338–2348 (2006).
- 812 89. Vogel, J. & Papenfort, K. Small non-coding RNAs and the bacterial outer  
813 membrane. *Current Opinion in Microbiology* **9**, 605–611 (2006).
- 814 90. Valentin-Hansen, P., Johansen, J. & Rasmussen, A. A. Small RNAs controlling  
815 outer membrane porins. *Current Opinion in Microbiology* **10**, 152–155 (2007).
- 816 91. Delihas, N. & Forst, S. MicF: an antisense RNA gene involved in response of  
817 *Escherichia coli* to global stress factors. *Journal of Molecular Biology* **313**, 1–12  
818 (2001).
- 819 92. Andersen, J. & Delihas, N. *micF* RNA binds to the 5' end of *ompF* mRNA and to a  
820 protein from *Escherichia coli*. *Biochemistry* **29**, 9249–9256 (1990).
- 821 93. Delihas, N. Discovery and characterization of the first non-coding RNA that  
822 regulates gene expression, *micF* RNA: A historical perspective. *World J Biol*  
823 *Chem* **6**, 272–280 (2015).
- 824 94. Inouye, M. The first demonstration of RNA interference to inhibit mRNA function.  
825 *Gene* **592**, 332–333 (2016).
- 826 95. Ramani, N., Hedeshian, M. & Freundlich, M. *micF* antisense RNA has a major  
827 role in osmoregulation of OmpF in *Escherichia coli*. *J Bacteriol* **176**, 5005–5010  
828 (1994).
- 829 96. Chou, J. H., Greenberg, J. T. & Demple, B. Posttranscriptional repression of  
830 *Escherichia coli* OmpF protein in response to redox stress: positive control of the  
831 *micF* antisense RNA by the *soxRS* locus. *J Bacteriol* **175**, 1026–1031 (1993).

- 832 97. Chen, S., Zhang, A., Blyn, L. B. & Storz, G. MicC, a second small-RNA regulator  
833 of Omp protein expression in *Escherichia coli*. *J Bacteriol* **186**, 6689–6697  
834 (2004).
- 835 98. Dam, S., Pagès, J.-M. & Masi, M. Dual regulation of the small RNA MicC and the  
836 quiescent porin OmpN in response to antibiotic stress in *Escherichia coli*.  
837 *Antibiotics (Basel)* **6**, (2017).
- 838 99. Blair, J. M. A., Webber, M. A., Baylay, A. J., Ogbolu, D. O. & Piddock, L. J. V.  
839 Molecular mechanisms of antibiotic resistance. *Nat. Rev. Microbiol.* **13**, 42–51  
840 (2015).
- 841 100. Du, D. *et al.* Multidrug efflux pumps: structure, function and regulation. *Nature*  
842 *Reviews Microbiology* **16**, 523 (2018).
- 843 101. Davin-Regli, A. *et al.* Membrane permeability and regulation of drug “influx and  
844 efflux” in enterobacterial pathogens. *Curr Drug Targets* **9**, 750–759 (2008).
- 845 102. Dupont, H. *et al.* Structural alteration of OmpR as a source of ertapenem  
846 resistance in a CTX-M-15-producing *Escherichia coli* O25b:H4 sequence type  
847 131 clinical isolate. *Antimicrobial Agents and Chemotherapy* **61**, e00014-17  
848 (2017).
- 849 103. Dupont, H. *et al.* Molecular characterization of carbapenem-nonsusceptible  
850 enterobacterial isolates collected during a prospective interregional survey in  
851 France and susceptibility to the novel ceftazidime-avibactam and aztreonam-  
852 avibactam combinations. *Antimicrobial Agents and Chemotherapy* **60**, 215–221  
853 (2016).
- 854 104. Tran, Q.-T. *et al.* Implication of porins in  $\beta$ -lactam resistance of *Providencia*  
855 *stuartii*. *J Biol Chem* **285**, 32273–32281 (2010).
- 856 105. Tran, Q.-T. *et al.* Porin flexibility in *Providencia stuartii*: cell-surface-exposed  
857 loops L5 and L7 are markers of *Providencia* porin OmpPst1. *Research in*  
858 *Microbiology* **168**, 685–699 (2017).
- 859 106. Oteo, J. *et al.* Emergence of imipenem resistance in clinical *Escherichia coli*  
860 during therapy. *International Journal of Antimicrobial Agents* **32**, 534–537 (2008).
- 861 107. Philippe, N. *et al.* *In vivo* evolution of bacterial resistance in two cases of  
862 *Enterobacter aerogenes* infections during treatment with imipenem. *PLoS One*  
863 **10**, (2015).

- 864 108. Lázaro-Perona, F. *et al.* Genomic path to pandrug resistance in a clinical  
865 isolate of *Klebsiella pneumoniae*. *International Journal of Antimicrobial Agents* **52**,  
866 713–718 (2018).
- 867 109. Yang, F.-C., Yan, J.-J., Hung, K.-H. & Wu, J.-J. Characterization of  
868 ertapenem-resistant *Enterobacter cloacae* in a Taiwanese University Hospital. *J*  
869 *Clin Microbiol* **50**, 223–226 (2012).
- 870 110. Fernández, J., Guerra, B. & Rodicio, M. R. Resistance to carbapenems in non-  
871 typhoidal *Salmonella enterica* Serovars from humans, animals and food. *Vet Sci*  
872 **5**, (2018).
- 873 111. Doumith, M., Ellington, M. J., Livermore, D. M. & Woodford, N. Molecular  
874 mechanisms disrupting porin expression in ertapenem-resistant *Klebsiella* and  
875 *Enterobacter* spp. clinical isolates from the UK. *J. Antimicrob. Chemother.* **63**,  
876 659–667 (2009).
- 877 112. Wozniak, A. *et al.* Porin alterations present in non-carbapenemase-producing  
878 *Enterobacteriaceae* with high and intermediate levels of carbapenem resistance  
879 in Chile. *Journal of Medical Microbiology* **61**, 1270–1279 (2012).
- 880 113. Cerqueira, G. C. *et al.* Multi-institute analysis of carbapenem resistance  
881 reveals remarkable diversity, unexplained mechanisms, and limited clonal  
882 outbreaks. *Proc Natl Acad Sci U S A* **114**, 1135–1140 (2017).
- 883 114. Novais, Â. *et al.* Spread of an OmpK36-modified ST15 *Klebsiella pneumoniae*  
884 variant during an outbreak involving multiple carbapenem-resistant  
885 *Enterobacteriaceae* species and clones. *Eur J Clin Microbiol Infect Dis* **31**, 3057–  
886 3063 (2012).
- 887 115. Shin, S. Y. *et al.* Resistance to carbapenems in sequence type 11 *Klebsiella*  
888 *pneumoniae* is related to DHA-1 and loss of OmpK35 and/or OmpK36. *Journal of*  
889 *Medical Microbiology* **61**, 239–245 (2012).
- 890 116. Martínez-Martínez, L. Extended-spectrum beta-lactamases and the  
891 permeability barrier. *Clin. Microbiol. Infect.* **14 Suppl 1**, 82–89 (2008).
- 892 117. Thiolas, A., Bollet, C., Scola, B. L., Raoult, D. & Pagès, J.-M. Successive  
893 emergence of *Enterobacter aerogenes* strains resistant to imipenem and colistin  
894 in a patient. *Antimicrobial Agents and Chemotherapy* **49**, 1354–1358 (2005).
- 895 118. Lavigne, J.-P. *et al.* An adaptive response of *Enterobacter aerogenes* to  
896 imipenem: regulation of porin balance in clinical isolates. *International Journal of*  
897 *Antimicrobial Agents* **41**, 130–136 (2013).

- 898 119. Lavigne, J.-P. *et al.* Membrane permeability, a pivotal function involved in  
899 antibiotic resistance and virulence in *Enterobacter aerogenes* clinical isolates.  
900 *Clinical Microbiology and Infection* **18**, 539–545 (2012).
- 901 120. Hamzaoui, Z. *et al.* An outbreak of NDM-1-producing *Klebsiella pneumoniae*,  
902 associated with OmpK35 and OmpK36 porin loss in Tunisia. *Microbial Drug*  
903 *Resistance* **24**, 1137–1147 (2018).
- 904 121. Gröbner, S. *et al.* Emergence of carbapenem-non-susceptible extended-  
905 spectrum  $\beta$ -lactamase-producing *Klebsiella pneumoniae* isolates at the university  
906 hospital of Tübingen, Germany. *Journal of Medical Microbiology* **58**, 912–922  
907 (2009).
- 908 122. Findlay, J., Hamouda, A., Dancer, S. J. & Amyes, S. G. B. Rapid acquisition of  
909 decreased carbapenem susceptibility in a strain of *Klebsiella pneumoniae* arising  
910 during meropenem therapy. *Clinical Microbiology and Infection* **18**, 140–146  
911 (2012).
- 912 123. Knopp, M. & Andersson, D. I. Amelioration of the fitness costs of antibiotic  
913 resistance due to reduced outer membrane permeability by upregulation of  
914 alternative porins. *Mol Biol Evol* **32**, 3252–3263 (2015).
- 915 124. Nelson, K. *et al.* Resistance to ceftazidime-avibactam is due to transposition of  
916 KPC in a porin-deficient strain of *Klebsiella pneumoniae* with increased efflux  
917 activity. *Antimicrobial Agents and Chemotherapy* **61**, e00989-17 (2017).
- 918 125. Shen, Z. *et al.* High ceftazidime hydrolysis activity and porin OmpK35  
919 deficiency contribute to the decreased susceptibility to ceftazidime/avibactam in  
920 KPC-producing *Klebsiella pneumoniae*. *J Antimicrob Chemother* **72**, 1930–1936  
921 (2017).
- 922 126. Pagès, J.-M., Peslier, S., Keating, T. A., Lavigne, J.-P. & Nichols, W. W. Role  
923 of the outer membrane and porins in susceptibility of  $\beta$ -lactamase-producing  
924 *Enterobacteriaceae* to ceftazidime-avibactam. *Antimicrob. Agents Chemother.* **60**,  
925 1349–1359 (2016).
- 926 127. Balabanian, G., Rose, M., Manning, N., Landman, D. & Quale, J. Effect of  
927 porins and *bla*<sub>KPC</sub> expression on activity of imipenem with relebactam in *Klebsiella*  
928 *pneumoniae*: Can antibiotic combinations overcome resistance? *Microbial Drug*  
929 *Resistance* **24**, 877–881 (2018).

- 930 128. Sun, D., Rubio-Aparicio, D., Nelson, K., Dudley, M. N. & Lomovskaya, O.  
931 Meropenem-vaborbactam resistance selection, resistance prevention, and  
932 molecular mechanisms in mutants of KPC-producing *Klebsiella pneumoniae*.  
933 *Antimicrob. Agents Chemother.* **61**, (2017).
- 934 129. Lunha, K. *et al.* High-level carbapenem-resistant OXA-48-producing *Klebsiella*  
935 *pneumoniae* with a novel OmpK36 variant and low-level, carbapenem-resistant,  
936 non-porin-deficient, OXA-181-producing *Escherichia coli* from Thailand.  
937 *Diagnostic Microbiology and Infectious Disease* **85**, 221–226 (2016).
- 938 130. Dé, E. *et al.* A new mechanism of antibiotic resistance in *Enterobacteriaceae*  
939 induced by a structural modification of the major porin. *Molecular Microbiology*  
940 **41**, 189–198 (2001).
- 941 131. Thiolas, A., Bornet, C., Davin-Régli, A., Pagès, J.-M. & Bollet, C. Resistance to  
942 imipenem, cefepime, and cefpirome associated with mutation in Omp36  
943 osmoporin of *Enterobacter aerogenes*. *Biochemical and Biophysical Research*  
944 *Communications* **317**, 851–856 (2004).
- 945 132. García-Fernández, A. *et al.* An ertapenem-resistant extended-spectrum- $\beta$ -  
946 lactamase-producing *Klebsiella pneumoniae* clone carries a novel OmpK36 porin  
947 variant. *Antimicrobial Agents and Chemotherapy* **54**, 4178–4184 (2010).
- 948 133. Clancy, C. J. *et al.* Mutations of the ompK36 porin gene and promoter impact  
949 responses of sequence type 258, KPC-2-producing *Klebsiella pneumoniae*  
950 strains to doripenem and doripenem-colistin. *Antimicrob Agents Chemother* **57**,  
951 5258–5265 (2013).
- 952 134. Papagiannitsis, C. C. *et al.* OmpK35 and OmpK36 porin variants associated  
953 with specific sequence types of *Klebsiella pneumoniae*. *Journal of Chemotherapy*  
954 **25**, 250–254 (2013).
- 955 135. Hall, J. M., Corea, E., Sanjeevani, H. D. A. & Inglis, T. J. J. Molecular  
956 mechanisms of  $\beta$ -lactam resistance in carbapenemase-producing *Klebsiella*  
957 *pneumoniae* from Sri Lanka. *Journal of Medical Microbiology* **63**, 1087–1092  
958 (2014).
- 959 136. Partridge, S. R. *et al.* Emergence of *bla*<sub>KPC</sub> carbapenemase genes in Australia.  
960 *International Journal of Antimicrobial Agents* **45**, 130–136 (2015).

- 961 137. García-Sureda, L. *et al.* OmpK26, a novel porin associated with carbapenem  
962 resistance in *Klebsiella pneumoniae*. *Antimicrob Agents Chemother* **55**, 4742–  
963 4747 (2011).
- 964 138. Bialek-Davenet, S. *et al.* *In-vivo* loss of carbapenem resistance by extensively  
965 drug-resistant *Klebsiella pneumoniae* during treatment via porin expression  
966 modification. *Sci Rep* **7**, (2017).
- 967 139. Kaczmarek, F. M., Dib-Hajj, F., Shang, W. & Gootz, T. D. High-level  
968 carbapenem resistance in a *Klebsiella pneumoniae* clinical isolate is due to the  
969 combination of *bla*<sub>ACT-1</sub>  $\beta$ -lactamase production, porin OmpK35/36 insertional  
970 inactivation, and down-regulation of the phosphate transport porin PhoE.  
971 *Antimicrobial Agents and Chemotherapy* **50**, 3396–3406 (2006).
- 972 140. Doménech-Sánchez, A., Hernández-Allés, S., Martínez-Martínez, L., Benedí,  
973 V. J. & Albertí, S. Identification and characterization of a new porin gene of  
974 *Klebsiella pneumoniae*: Its role in  $\beta$ -lactam antibiotic resistance. *J Bacteriol* **181**,  
975 2726–2732 (1999).
- 976 141. Castanheira, M., Mendes, R. E. & Sader, H. S. Low frequency of ceftazidime-  
977 avibactam resistance among *Enterobacteriaceae* isolates carrying *bla*<sub>KPC</sub>  
978 collected in U.S. hospitals from 2012 to 2015. *Antimicrob Agents Chemother* **61**,  
979 (2017).
- 980 142. Noinaj, N., Gumbart, J. C. & Buchanan, S. K. The  $\beta$ -barrel assembly  
981 machinery in motion. *Nat Rev Microbiol* **15**, 197–204 (2017).
- 982 143. Schiffrin, B., Brockwell, D. J. & Radford, S. E. Outer membrane protein folding  
983 from an energy landscape perspective. *BMC Biol* **15**, (2017).
- 984 144. Robinson, J. A. Folded synthetic peptides and other molecules targeting outer  
985 membrane protein complexes in Gram-negative bacteria. *Front Chem* **7**, (2019).
- 986 145. Hao, M. *et al.* Porin deficiency in carbapenem-resistant *Enterobacter*  
987 *aerogenes* strains. *Microbial Drug Resistance* **24**, 1277–1283 (2018).
- 988 146. Jiménez-Castellanos, J.-C. *et al.* Envelope proteome changes driven by RamA  
989 overproduction in *Klebsiella pneumoniae* that enhance acquired  $\beta$ -lactam  
990 resistance. *J. Antimicrob. Chemother.* **73**, 88–94 (2018).

991 147. Chetri, S. *et al.* Transcriptional response of OmpC and OmpF in *Escherichia*  
 992 *coli* against differential gradient of carbapenem stress. *BMC Research Notes* **12**,  
 993 138 (2019).

994

995 **BOXES REFERENCES**

996 148. Bhamidimarri, S. P., Prajapati, J. D., van den Berg, B., Winterhalter, M. &  
 997 Kleinekathöfer, U. Role of electroosmosis in the permeation of neutral molecules:  
 998 CymA and cyclodextrin as an example. *Biophys J* **110**, 600–611 (2016).

999 149. Talbot, G. H.  $\beta$ -Lactam antimicrobials: what have you done for me lately?  
 1000 *Annals of the New York Academy of Sciences* **1277**, 76–83 (2013).

1001 150. Olivares, J. *et al.* The intrinsic resistome of bacterial pathogens. *Front*  
 1002 *Microbiol* **4**, (2013).

1003 151. Li, X.-Z., Plésiat, P. & Nikaido, H. The challenge of efflux-mediated antibiotic  
 1004 resistance in Gram-negative bacteria. *Clin Microbiol Rev* **28**, 337–418 (2015).

1005 152. Xia, J., Gao, J. & Tang, W. Nosocomial infection and its molecular  
 1006 mechanisms of antibiotic resistance. *BioScience Trends* **10**, 14–21 (2016).

1007 153. Nikaido, H. & Pagès, J.-M. Broad specificity efflux pumps and their role in  
 1008 multidrug resistance of Gram negative bacteria. *FEMS Microbiol Rev* **36**, 340–  
 1009 363 (2012).

1010 154. Davin-Regli, A., Lavigne, J.-P. & Pagès, J.-M. *Enterobacter* spp.: Update on  
 1011 taxonomy, clinical aspects, and emerging antimicrobial resistance. *Clinical*  
 1012 *Microbiology Reviews* **32**, e00002-19 (2019).

1013 155. Pagès, J.-M. *et al.* Efflux Pump, the masked side of  $\beta$ -Lactam resistance in  
 1014 *Klebsiella pneumoniae* clinical isolates. *PLOS ONE* **4**, e4817 (2009).

1015 156. Westfall, D. A. *et al.* Bifurcation kinetics of drug uptake by Gram-negative  
 1016 bacteria. *PLOS ONE* **12**, e0184671 (2017).

1017 157. Nicolas-Chanoine, M.-H., Mayer, N., Guyot, K., Dumont, E. & Pagès, J.-M.  
 1018 Interplay between membrane permeability and enzymatic barrier leads to  
 1019 antibiotic-dependent resistance in *Klebsiella pneumoniae*. *Front Microbiol* **9**,  
 1020 (2018).

1021 158. Wan Nur Ismah, W. A. K., Takebayashi, Y., Findlay, J., Heesom, K. J. &  
 1022 Avison, M. B. Impact of OqxR loss of function on the envelope proteome of



- 1023 *Klebsiella pneumoniae* and susceptibility to antimicrobials. *J Antimicrob*  
1024 *Chemother* **73**, 2990–2996 (2018).
- 1025 159. Castanheira, M. *et al.* Analyses of a ceftazidime-avibactam-resistant  
1026 *Citrobacter freundii* isolate carrying *bla*<sub>KPC-2</sub> reveals a heterogenous population  
1027 and reversible genotype. *mSphere* **3**, (2018).
- 1028 160. Fajardo-Lubián, A., Ben Zakour, N. L., Agyekum, A., Qi, Q. & Iredell, J. R.  
1029 Host adaptation and convergent evolution increases antibiotic resistance without  
1030 loss of virulence in a major human pathogen. *PLoS Pathog* **15**, (2019).
- 1031 161. Nikaido, H. Role of permeability barriers in resistance to  $\beta$ -lactam antibiotics.  
1032 *Pharmacology & Therapeutics* **27**, 197–231 (1985).

1033

1034 **FIGURES REFERENCE**

1035

- 1036 162 Coines, J., Acosta-Gutierrez, S., Bodrenko, I., Rovira, C. & Ceccarelli, M.  
1037 Glucose transport via the pseudomonads porin OprB. Implications for the design  
1038 of Trojan-horse antinfectives. *Phys. Chem. Chem. Phys.* **21**, 8457–8463 (2019).

1039

## FIGURE LEGENDS

### Figure 1: Structural aspects of enterobacterial porins

Extracellular (a) and side views (b) of the OmpC trimer, with L2 coloured green and the pore-constricting loop L3 coloured magenta. Loops have been smoothed for clarity. OM, outer membrane. c, d Extracellular (c) and slabbed side views (d) of an OmpC monomer with the residues lining the eyelet of the constriction region (CR) shown by stick models. e, Cross-section through OmpC showing the internal funnel-like shape of the channel coloured by electrostatic potential. The constriction region (CR) is indicated. f, View as in e, but close-up and with residues on both sides of the CR shown as stick models.

### Figure 2: Structural differences in enterobacterial porins have implications for permeation and antibiotic resistance.

Superposed cartoon views for OmpC orthologs from *E. coli* (a), *K. pneumoniae* (b) and *E. aerogenes* (c). The bottom row shows the corresponding OmpF orthologs (d-f). The eyelet-lining residues equivalent to K16, R37, R74, R124, D105 and E109 of *E. coli* OmpC are shown as grey stick models. These key residues are identical in Enterobacterial porins. Examples of equivalent residues near the constriction zone that differ between OmpC and OmpF proteins are labeled and shown as yellow stick models (e.g. Q33, W72, G116 and K317 in *E. coli* OmpC, M38, K80, Y124 and I314 in *E. coli* OmpF). Subtle differences in structure such as these can lead to alteration of the electric field close to and within the constriction zone, which in turn can result in a decreased translocation efficacy of antibiotic across the channel, thus contributing to the emergence of resistance.

### Figure 3: Mechanism of translocation/Permeation model of molecules through general porins.

The translocation of the zwitterionic meropenem through OmpF. Shown in red surface are the acidic residues of loop L3 and in blue surface the residues of the basic ladder. Loop L3 is shown in magenta. The colored spheres indicate the carboxylic and the amine group (pyrrolidine) of meropenem, respectively in red and blue. The colored arrows represent the electric dipole moment of meropenem.

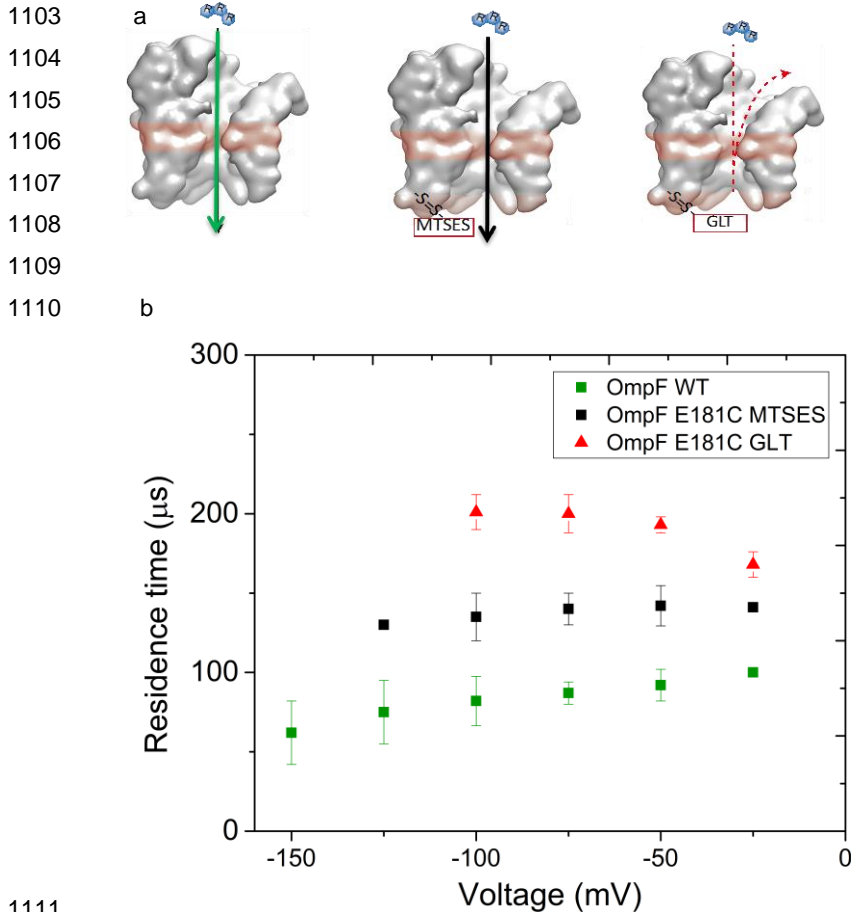
1074 Recent results suggest a free energy landscape model for the passive diffusion of  
 1075 molecules through porins from *Enterobacteriaceae*, as depicted in the figure. The  
 1076 downward diffusion of meropenem in the constriction region, highlighted as a  
 1077 rectangular box, starts by (arrow orange) attraction of the carboxylic group towards  
 1078 the residues R167-R168; (arrow pink) alignment of the dipole to the transversal  
 1079 electric field in the preorientation region with the amine group pointing toward the  
 1080 loop L3; (arrow yellow) sliding of the meropenem in the CR maintaining the dipole  
 1081 aligned with the transversal electric field, with the carboxylic group along the basic  
 1082 ladder and the amine group pointing the loop L3; (arrow green) exit of the  
 1083 meropenem from the CR by rotation of the dipole<sup>66</sup>. Since the porins are  
 1084 characterized by an hourglass shape, a steric barrier will be always present (black  
 1085 energy profile), strongly limiting the permeability. In order to increase the flux an  
 1086 electrostatic compensation of the barrier is needed<sup>58</sup> (orange dotted energy profile),  
 1087 which occurs when the dipole moment of the molecule aligns with the transversal  
 1088 electric field inside the pore (yellow arrow of meropenem). On the other hand, if the  
 1089 electrostatic interactions create a strong binding site as in substrate-specific  
 1090 channels, as it may happen in the preorientation region<sup>33</sup> (pink arrow), the pore might  
 1091 reach saturation and the increase of the flux would be limited at high  
 1092 concentration<sup>162</sup>. In the limit of low concentration, the flux at concentration gradient  
 1093  $\Delta C$  is quantified in terms of the permeability coefficient through a single pore  $P$ ,  
 1094 calculated knowing the potential of mean force  $F(z)$  (molecule-pore-water interaction)  
 1095 and the diffusion constant of the molecule inside the pore  $D(z)$ . **Only when**  
 1096 considering the complete interaction of the molecule inside the entire pore (to note  
 1097 the integral over the pore length  $L$ ) it would be possible to predict the flux. This  
 1098 explains why early efforts using docking methods, via searching for local  
 1099 affinity/binding sites, failed to provide guidance rules for transport.

1100  
 1101

Commented [LM9]: And  $F(0)$  definition ?

Commented [MC10]:  $F(0)$  is the energy at the entry of the pore, I added it in the new Fig.3 as the indication of z-axis

1102 **BOX 1: Counting permeating molecules with an exit barrier.**



1111

1112

1113 Information on the contribution of the individual porin on permeation can be obtained

1114 via single channel reconstitution into planar lipid bilayer. The molecule needs to enter

1115 the channel and block the ion current sufficiently. To distinguish binding from

1116 translocation we apply external forces pushing or pulling the molecule while

1117 recording their residence time. For charged molecule we may use electric fields<sup>54,148</sup>.

1118 In the case of uncharged molecules, electro-osmosis can be considered<sup>148</sup>. The latter

1119 effect originates from excess of charged residues in the constriction zone: porins

1120 often are cation selective, which typically implies an excess of negatively charged

1121 residues at the channel surface combined with a cloud of mobile cationic

1122 counterions. Application of an external voltage will cause a flow of the counterions  
1123 along the field creating a net flow pushing molecules. Surprisingly this effect is quite  
1124 strong and comparable to diffusion already at  $\mu\text{M}$  concentration gradient.

1125 As an example to detect fast permeating molecules or to distinguish molecules which  
1126 permeate from those which only binds and reflects backwards, a barrier at the exit  
1127 has been engineered. Above we show an example of OmpF from *E. coli*. A single  
1128 point mutation in OmpF at position 181 OmpF<sup>E181C</sup> was introduced and crosslinked  
1129 with either the small blocker Sodium (2-sulfonatoethyl) MethaneThioSulfonate  
1130 (MTSES) or the large blocker glutathione (see the figure 1). Tri-arginine is a charged  
1131 molecule that is pulled into the channel under negative applied voltage. Tri-arginine  
1132 permeates efficiently through OmpF (see lhs in figure a) and could not be detected  
1133 previously, higher negative voltage leads to faster permeation (figure 1b, green  
1134 squares). The modification of OmpF<sup>E181C</sup> by MTSES creates a barrier at the exit that  
1135 is sufficient to alter the pathway of Tri-arginine (Arg-Arg-Arg), on average the  
1136 triarginine stays longer in the channel (figure 1b, black squares). In the case of GLT  
1137 (figure 1a, rhs), the molecule has to return against the electric field leading to a  
1138 pronounced residence time with increasing field strength (figure 1b, red triangles)<sup>5</sup>.  
1139 This approach might enable the discrimination of blockage events from translocation  
1140 events for a wide range of substrates while working in the  $\mu\text{M}$  range. As the data  
1141 analysis is straightforward, parallelisation of experiments might be possible. A  
1142 potential application of this technique could include screening for molecular  
1143 structures to improve the permeability of antibiotics.

1144

1145

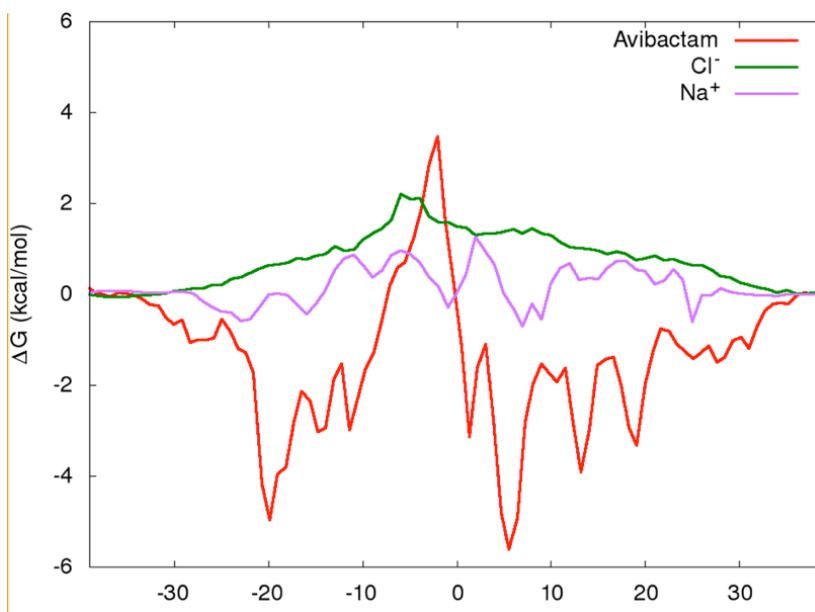
1146

**Commented [LM11]:** Maybe I m missing something  
:Does MTSES really block or it's more difficult to  
permeate. I find the legend does not explain well the  
differences between the two blockers.

1147 **BOX 2: Transport of charged compounds revealed by a concentration gradient.**

1148 Electrolyte solutions always contain an equal amount of charges. Application of a  
 1149 concentration gradient across the membrane results in a diffusion-driven flux. In most  
 1150 cases, one of the ions diffuses faster than the counter ion and the difference in flux  
 1151 creates a diffusion potential and provides information on the channel selectivity but  
 1152 not on the absolute flux. However, in combination with single channel conductance  
 1153 data it is possible to extract the true flux of the individual ions<sup>56</sup>.

1154



1155

1156 Computer modelling can nowadays predict the energy barrier of a molecule along the  
 1157 channel axis which allows to obtain an estimate for the flux. In the above figure we  
 1158 show the free-energy surface of avibactam along the Z axis of diffusion and, for a  
 1159 comparison with free energies of Cl<sup>-</sup> and Na<sup>+</sup> ions, calculated using their relative  
 1160 densities with respect to the bulk. Note that OmpF is slightly cation selective and the  
 1161 preference for cations is reflected by a slight affinity. In contrast anions are exposed  
 1162 to a shallow energy barrier. Avibactam has a narrow but high barrier in the middle  
 1163 combined with two affinity sites before and after the barrier<sup>56</sup>. We expect that in the  
 1164 near future such energy profiles can be obtained in a semi-automated manner from  
 1165 larger libraries which later may be experimentally identified.

Commented [LM12]: Need to be rephrased. Link between the two paragraphs of the box not clear. 'However, combination of single channel conductance data and molecular dynamics modelling provide information on the true flux of the individual ions '

Commented [LM13]: X axis missing: Z (Å)

1166 **BOX 3: Interplay between porin alteration,  $\beta$ -lactamase and efflux pump**  
1167 **activities in internal concentration of active antibiotics.**

1168

1169 It is now recognized that three key factors, - the outer membrane permeability, -the  
1170 enzymatic degradation and - the efflux pumps, efficiently govern the internal  
1171 concentration of active  $\beta$ -lactams close to its periplasmic target.

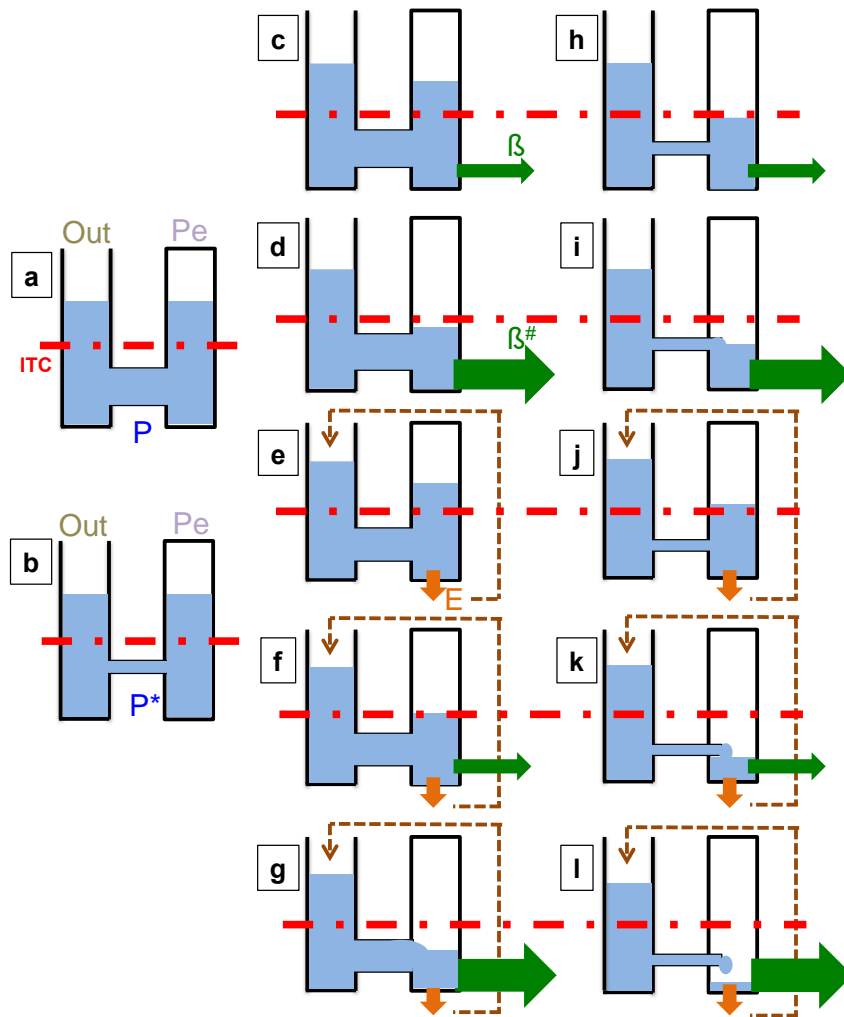
1172 Regarding the clinical isolates, these mechanisms acting alone or together drastically  
1173 alter the antibacterial spectrum of the molecule alone or the combination  $\beta$ -lactam +  
1174  $\beta$ -lactamase inhibitor used during patient treatment. Some possible clinical events  
1175 are illustrated in the following figure.

1176

1177 In medium column (**c,d,e,f,g**) the strains exhibit a normal porin expression, in  
1178 contrast right column (**h,i,j,k,l**) represent a altered porin phenotype (lack or mutation  
1179 of channel function). Several combinations are hypothesized in 'c' to 'l', for instance:  
1180 in 'i', porin alteration +  $\beta$ -lactamase overexpression generating a decrease of  $\beta$ -  
1181 lactam susceptibility, or in 'l' porin alteration +  $\beta$ -lactamase overexpression + efflux  
1182 conferring a total resistance. These well-combined strategies have been reported in  
1183 numerous *Klebsiella* or *Enterobacter* isolates and they strongly impair  $\beta$ -lactams  
1184 activities. It is important to note that a reduced penetration (porin alteration) and/or an  
1185 efflux activity strongly reinforce the effect of enzymatic barrier and, by side effect,  
1186 contribute to the induction of  $\beta$ -lactamase expression. This sophisticated  
1187 management used by the bacterial genius of internal concentration of active  $\beta$ -  
1188 lactams contributes to bacterial survival and therapeutic failure. For reviews see  
1189 99,100,149-154 and some recent selected papers<sup>126,138,146,155-160</sup>.

1190 It must be noted that a fraction of the expelled antibiotics can re-enter bacterial cell  
1191 (**dashed brown arrows**) for a second run in contrast to the  $\beta$ -lactams treated by  $\beta$ -  
1192 lactamases that are cleaved (**green arrows**).

1193



1194

1195

1196 **Legend:**1197 The antibiotic flux across the porin, from external medium (left column, **Out**) to1198 periplasmic space (right column, **Pe**), is illustrated by the channel joining the two



1199 compartments. The maximal diameter of the channel (**P in a**) represents the normal  
1200 wild type porin production (number of copies, normal conductance), the small  
1201 diameter (**P\* in b**) corresponds to a porin alteration (diminution of porin expression, a  
1202 change of porin type (OmpF > PhoE) or a mutation inducing an alteration of channel  
1203 properties in CR for instance). For reviews see <sup>5,65,99,100,138,150</sup>.

1204  $\beta$  indicates the presence of  $\beta$ -lactamases that cleave  $\beta$ -lactam molecules in  
1205 periplasmic space decreasing the number of active antibiotics and  $\beta^\#$  illustrates the  
1206 overproduction of  $\beta$ -lactamases (**green arrows**). **E** indicates the presence of active  
1207 efflux pumps that expel the antibiotic outside the bacterial cell <sup>6,17,146,150-155,158</sup>. The  
1208 antibiotic ejected by efflux pump (**E**) can re-enter bacterial cell (**dashed brown**  
1209 **arrows**) for a second try.

1210 **ITC** (for internal threshold concentration, **red dashed lane**) represents the theoretical  
1211 concentration necessary to inhibit the function of bacterial target. We have arbitrary  
1212 fixed the alteration of penetration (due to mutation or porin lack), the rate of  
1213 periplasmic hydrolysis and the effect of antibiotic efflux on internal antibiotic level.  
1214 The resulting level of antibiotic accumulation is only roughly estimated to give a  
1215 simple schema of the respective contributions of the three mechanisms.

1216 This figure is an upgrade of the pioneer H. Nikaido's model describing the interplay  
1217 "porin- $\beta$  lactamase" in resistance<sup>161</sup>.

1218